life

MDPI

Article

RETRACTED: Repurposing Diltiazem for Its Neuroprotective Anti-Dementia Role against Intra-Cerebroventricular Streptozotocin-Induced Sporadic Alzheimer's Disease-Type Rat Model

Ramesh Alluri [1,*], Eswar Kumar Kilari [2], Praveen Kumar Pasala [3], Spandana Rajendra Kopalli [4] and Sushruta Koppula [5,*]

1 Cognitive Science Research Initiative Lab., Department of Pharmacology, Vishnu Institute of Pharmaceutical Education and Research, Medak Dist., Narsapur 502313, India
2 Department of Pharmacology, University College of Pharmaceutical Sciences, Andhra University, Visakhapatnam 530003, India
3 Department of Pharmacology, Raghavendra Institute of Pharmaceutical Education and Research, Jawaharlal Nehru Technological University Anantapur—JNTUA, Anantapur 515721, India
4 Department of Integrated Bioscience and Biotechnology, Sejong University, Gwangjin-gu, Seoul 05006, Republic of Korea
5 College of Biomedical and Health Science, Konkuk University, Chungju-si 380-701, Republic of Korea
* Correspondence: rameshcology@gmail.com (R.A.); koppula@kku.ac.kr (S.K.); Tel.: +91-97-01683444 (R.A.); +82-43-8403609 (S.K.)

Abstract: Alzheimer's disease (AD) is an age-related neuropsychiatric disorder and a common cause of progressive dementia. Diltiazem (DTZ), the non-dihydropyridine benzothiazepine class of calcium channel blocker (CCB), used clinically in angina and other cardiovascular disorders, has proven neurological benefits. In the present study, the neuroprotective anti-dementia effects of DTZ against intra-cerebroventricular-streptozotocin (ICV-STZ)-induced sporadic AD (SAD)-type rat model was investigated. ICV-STZ-induced cognitive impairments were measured via passive avoidance and Morris water maze tasks. Anti-oxidative enzyme status, pro-inflammatory markers, and amyloid-beta (Aβ) protein expression in rat brain tissues were measured using ELISA kits, Western blotting, and immunostaining techniques. The data revealed that ICV-STZ injection in rats significantly induced cognitive deficits and altered the levels of oxidative and pro-inflammatory markers ($p < 0.05 \sim p < 0.001$). Treatment with DTZ (10 mg/kg, 20 mg/kg, and 40 mg/kg, p.o.) daily for twenty-one days, 1 h before a single ICV-STZ (3 mg/kg) injection, significantly improved cognitive impairments and ameliorated the ICV-STZ-induced altered nitrite, pro-inflammatory cytokines (TNF-α, and IL-1β) and anti-oxidative enzyme levels (superoxide dismutase, lipid peroxidation, and glutathione). Further, DTZ restored the increased Aβ protein expression in ICV-STZ-induced brain tissue. Considering the results obtained, DTZ might have a potential therapeutic role in treating and managing AD and related dementia pathologies due to its anti-dementia activity in SAD-type conditions in rats induced by ICV-STZ.

Keywords: Alzheimer's disease; diltiazem; intra-cerebroventricular; streptozotocin; cognition; amyloid beta; anti-oxidant enzymes

check for updates

Citation: Alluri, R.; Kilari, E.K.; Pasala, P.K.; Kopalli, S.R.; Koppula, S. RETRACTED: Repurposing Diltiazem for Its Neuroprotective Anti-Dementia Role against Intra-Cerebroventricular Streptozotocin-Induced Sporadic Alzheimer's Disease-Type Rat Model. *Life* **2023**, *13*, 1688. https://doi.org/10.3390/life13081688

Academic Editors: Juraj Javor and Ivana Shawkatová

Received: 8 July 2023
Revised: 2 August 2023
Accepted: 3 August 2023
Published: 4 August 2023
Retracted: 16 July 2026

Copyright: © 2023 by the authors. Licensee MDPI, Basel, Switzerland. This article is an open access article distributed under the terms and conditions of the Creative Commons Attribution (CC BY) license (https://creativecommons.org/licenses/by/4.0/).

1. Introduction

Alzheimer's disease (AD), the principal cause of senile dementia, is a progressive neurodegenerative disease that distresses millions of patients over 65 years of age worldwide [1,2]. The deposition of β-amyloid (Aβ) senile plaques, neurofibrillary tangles, tau hyperphosphorylation, and cognitive dysfunctions are the well-accepted hallmarks of AD [3]. Although the familial type of AD constitutes up to five percent of AD cases, the

This paper has been retracted. A retraction notice was published on 16 July 2026 in *Life* **2026**, *16*, 1175. https://doi.org/10.3390/life16071175

majority type found is late-onset sporadic AD (SAD) [4]. SAD involves key etiopathogenic mechanisms, including environmental, metabolic, genetic, and lifestyle factors causing numerous disturbances, including chronic oxidative stress, cholinergic deficits, and neuroinflammation [5]. Currently, available medications for the treatment of AD, such as galantamine, rivastigmine, donepezil, and memantine, are symptomatic and offer limited therapeutic advantages and do not prevent disease progression [6].

The concept of drug repurposing by investigating established and old drugs used for other pharmacological benefits for the treatment of neurodegenerative diseases holds great potential [7]. Calcium channel blockers (CCBs) clinically used as antihypertensive and antianginal agents are being used by millions of patients in a safe and efficacious manner [8]. The broad array of epidemiologic data and translational science revealed a promising approach for CCBs to be repurposed for neuroprotection and delay progressive neurodegenerative disorders [9–11]. Previous studies suggested that CCBs exhibited promising effects as therapeutics for treating AD [12]. Calcium has been linked with cognitive function, neural plasticity, and neuronal physiology [13]. Calcium imbalance and/or dysregulation is observed in the course of human aging and neurological disorders, including AD [14–16]. Evidence suggests that CCBs such as memantine, nimodipine, and verapamil are efficacious for treating AD by targeting receptor-operated calcium channels and voltage-gated calcium channels, thereby protecting AD cells from Aβ oligomer production in various in vitro and in vivo animal models [17–19]. Further, several other classes of CCBs, including nicardipine, felodipine, and nifedipine, ameliorated memory deficits associated with hypoxic conditions [20,21].

CCBs were well documented to possess immense anti-oxidant and anti-inflammatory effects [11,22–24]. Diltiazem (DTZ), a benzothiazepine class of voltage-gated CCB clinically used in angina and in the treatment of cardiovascular diseases, exhibited various pharmacological benefits in experimental models [25,26]. DTZ exhibited protective effects against traumatic brain injury, cyanide-induced neurotoxicity, anti-inflammation, pentylenetetrazole-provoked amnesia, glutamate-induced excitotoxicity in an ischemia model, a spinal cord ischemia–reperfusion injury rabbit model, aluminum chloride-induced dementia, and lead toxicity [27–33]. Further, DTZ, by blocking Ca^{2+}, is known to reduce the adverse effects of calcium dysregulation and has been proposed to be useful in AD [17,34]. However, the neuroprotective anti-dementia role and its underlying mechanisms of DTZ in sporadic AD-type conditions in experimental models were not documented.

Streptozotocin (STZ), a glucosamine–nitrosourea combination widely used in laboratory animals to induce diabetes, was reported to cause serious damage to the brain and other metabolic irregularities in the central nervous system (CNS) [35]. Further, reports indicated that intra-cerebrovascular (ICV) injection of STZ impairs glucose and energy metabolism in the CNS, triggering neurodegeneration [36,37]. ICV injection of STZ increases β-amyloid protein expression, cognitive deficits, chronic neuroinflammation, anxiety, and increased oxidative stress and is identified as a classical model featuring SAD [38,39]. Given such reports, in the present study, DTZ was investigated for its neuroprotective role against ICV-STZ-induced SAD type model in rats. In addition, the pharmacological effect of DTZ on ICV-STZ-induced anti-oxidative defense factors, neuroinflammatory cytokines, and the expression of Aβ in the tissues of rat brains was also investigated.

2. Materials and Methods

2.1. Chemicals

The following analytical reagents were obtained from Sigma (St. Louis, MO, USA): DTZ (Figure 1A), 5,5′-Dithiobis-2-nitrobenzoic acid (DTNB), STZ, glutathione (GSH), 2-thiobarbituric acid (TBA), phosphate-buffered saline (PBS), and bovine serum albumin (BSA). Immunohistochemistry and Western blotting antibodies were purchased from Invitrogen in Camarillo, CA, USA. Fresh drug solutions were prepared before administration.

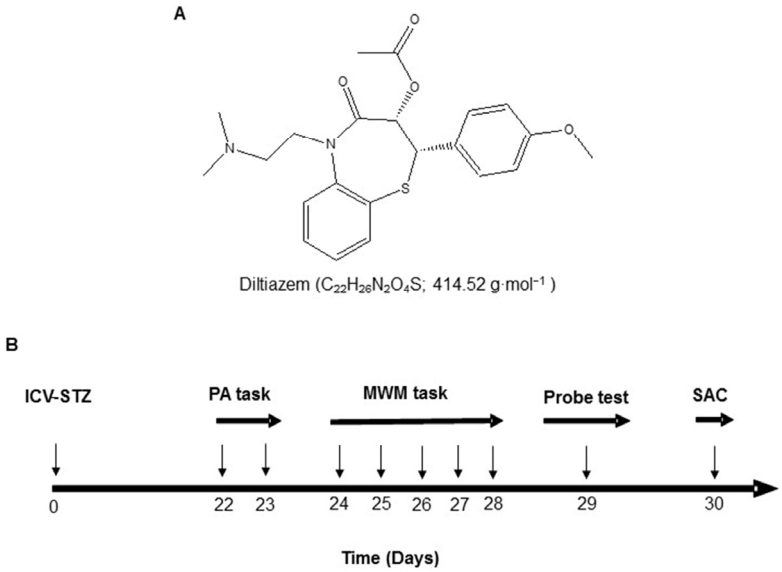


Figure 1. (**A**) Structure, chemical formula, and molar mass of DTZ. (**B**) The method of treatment, the intervals for estimating different parameters, and the experimental design. ICV-STZ: intracerebroventricularstreptozotocin, DTZ: diltiazem, MWM: Morris water maze, PA: passive avoidance, SAC: sacrificed.

2.2. Animals

Wistar rats of either sex (36 males and 36 females) weighing 150–200 g and aged 8 to 12 weeks were used for this study. The animals were kept in colony cages at our facility's Central Animal House, which had unlimited access to a standard mouse pelleted-diet and water and had a 12 h light/dark cycle, an ambient temperature of 25 ± 2 °C, and a relative humidity of 45–55%. Each study followed the guidelines set forth by our Institutional Animal Care and Use Committee (No. 1358/ac/10/CPCSEA) and the "Purpose of Control and Supervision of Experiments on Animals" (CPCSEA).

2.3. Surgical Procedures and ICV-STZ Treatment

STZ was administered via the ICV route, as previously stated, with a minor change [36]. Animals were made unconscious via intraperitoneal (i.p.) injections of ketamine hydrochloride (70 mg/kg, i.p.) and diazepam (4 mg/kg, i.p.). After thoroughly cleaning the region with povidone–iodine alcoholic solution, the animal was placed on the operating table, the head was straightened, the hair was trimmed, and a midline sagittal scalp incision was made. The coordinates for ICV-STZ injections were followed according to our previous report [40]. Artificial cerebrospinal fluid (ACSF; 2.9 mM KCl; 147 mM NaCl, 1.7 mM $CaCl_2$, 1.6 mM $MgCl_2$, and 2.2 mM dextrose) containing STZ (3 mg/kg b.w.) was injected ICV into the lesioned groups on both sides. Similar procedures were performed on the control group, but ACSF was administered in the same volume in place of STZ. Rats were placed on a heated pad throughout the procedure and recovery period. The rats were kept in individual cages for recovery until they resumed their normal behavior.

2.4. Experimental Design

After a week of adaptation, the animals were randomly divided into six groups (n = 12). Control Group I received a single injection of ACSF through an ICV line and treated with vehicle (PBS) for 21 days, and group II received a single infusion of STZ (3 mg/kg ICV) on day one and treated with vehicle (PBS) for 21 days. Subjects in Groups III, IV, and V were administered a single dose of STZ (3 mg/kg, ICV) on day 1, followed by 21 days of treatment with DTZ (10, 20, and 40 mg/kg/day, respectively) administered orally (p.o.). Group VI received a single infusion of STZ (3 mg/kg, ICV) on day 1, followed by 21 days of treatment with a standard drug, donepezil (0.1 mg/kg, p.o.). DTZ and donepezil were

dissolved in a vehicle (PBS), and the concentration was set to 10 mL/kg b.w. After three weeks of STZ or ACSF infusions, the animals underwent behavioral and biochemical assessments. The body weights of all groups were noted in pre- and post-experimental schedules. The experimental design and treatment schedule are depicted in Figure 1B.

2.5. Behavioral Studies

Behavioral assessments were carried out beginning in the fourth week following ICV-STZ infusion and the subsequent administration of DTZ or DON, as previously described [40].

2.5.1. Passive Avoidance Test

The memory retention deficits in ICV-STZ-induced rats were performed on days 22 and 23 using a passive avoidance test [41]. Briefly, the instrument consists of two independent chambers joined by a guillotine door. One of the areas was illuminated, whereas the other remained dark. The floors of both chambers have steel grids, which are used to deliver electric foot shocks (75 V; 0.2 mA, 50 Hz). The design of the equipment and the experimental procedures involving the acquisition and retention trials for each rat and the recording of the latency times were performed as described in our previous study [40]. Short latencies imply poor retention.

2.5.2. Morris Water Maze (MWM) Test

Following the passive avoidance test, the MWM task was conducted to assess the special learning and memory abilities of the animals as described earlier [42]. Briefly, the MWM apparatus contains a cylindrical water tank with a diameter of 130 cm and a height of 62 cm, filled with water to a depth of 40 cm (at a temperature of 25 ± 2 °C). The water was made cloudy with non-toxic paint. The pool was partitioned into four equitably sized quadrants, denoted as North, South, East, and West. A concealed escape platform with a diameter of 10 cm was positioned at a fixed location within one of the quadrants, submerged 2 cm beneath the water's surface. The platform remains in the same quadrant throughout the duration of the experiment. Prior to the start of the training, rats were allowed to swim freely in the pool with the platform for 60 s. Upon ascending the platform, the animal maintained its position for a duration of 30 s prior to the commencement of the subsequent trial. If a rat took longer than 60 s to find and reach the escape platform, it was carefully placed on the platform and allowed to stay there for the same amount of time. Latency times (in seconds) were recorded for each platform. A probing test was conducted 24 h following the acquisition phase by removing the platform. Rats were allowed to swim freely in the pool for 60 s. The amount of time spent in the target quadrant, which formerly housed the hidden platform, was recorded. The amount of time spent in the intended quadrant represents the extent of consolidation of memory experienced after learning.

2.6. Biochemical Analysis

2.6.1. Tissue Préparations

Rats were deeply euthanized under ketamine (150 mg/kg) anesthesia for 24 h following the MWM tests, and their brains were taken immediately and preserved on ice on a glass plate. The hippocampus and cerebral cortex were removed using the rat brain matrix and the rat brain atlas [43]. Six brains were hemisected across the center and frozen on dry ice for preservation. The tissues in one hemisphere were homogenized in lysis buffer for use in WB, and the tissues in the other hemisphere were independently homogenized in 10 mM tris-buffer (pH 7.4) with protease inhibitors. In order to estimate lipid peroxidation (LPO), the nuclear debris was separated from the homogenate by centrifuging it at 800× *g* for 5 min at 4 °C. The supernatant was further centrifuged at 10,000× *g* for 20 min at 4 °C to obtain post-mitochondrial supernatant (PMS), which was utilized for additional biochemical tests. After transcardial perfusion with saline and 4% paraformaldehyde, the brains of the remaining six rats in each group were removed and either fixed in 3.7%

formaldehyde in PBS 1X solution, embedded in paraffin and then 5 µm sections were cut for immunohistochemistry.

2.6.2. Measurement of LPO

The quantitative measurement of thiobarbituric acid-reactive species (TBARS), an indicator of lipid peroxidation in the brain, was evaluated as described previously [44].

2.6.3. Measurement of Brain GSH Levels

The brain GSH content was determined using the method outlined by Ellman [45]. The supernatant, measuring 1 mL, was subjected to precipitation using 1 mL of 4% sulfosalicylic acid. The resulting mixture was then cold-digested at a temperature of 4 °C for a duration of 1 h. The samples underwent centrifugation at a speed of 1200× *g* for a duration of 15 min at a temperature of 4 °C. To analyze the supernatant, a mixture was prepared by adding 2.7 mL of phosphate buffer (0.1 M, pH 8) and 0.2 mL of 5,5-dithio-bis (2-nitrobenzoic acid) to 1 mL of the supernatant. The yellow color that was produced was measured at a wavelength of 412 nm using a T60 UV/VIS spectrophotometer (PG Instruments Limited, Delhi, India).

2.6.4. Measurement of Superoxide Dismutase (SOD) Levels

SOD levels were measured by its ability to block the photochemical reduction of nitro blue tetrazolium (NBT), as stated previously [46]. Enzymatic activity was expressed in units per milligram of protein.

2.6.5. Effect on Brain Nitrite and Pro-Inflammatory Cytokine Levels

Nitric oxide (NO) production in the supernatant was measured as described previously [47]. Griess reagent and supernatant were mixed together in equal parts, and the resultant mixture was incubated for 10 min at room temperature in the dark, and a T60 UV/VIS spectrophotometer was used to measure the absorbance at 540 nm (PG Instruments Limited, Delhi, India). The nitrite concentration in the supernatant was calculated using a sodium nitrite standard curve and quantified as micromoles per milligram protein. To assess pro-inflammatory mediator levels, TNF-α and IL-1β levels were determined using respective immunoassay kits. Marker concentrations were calculated using standard curves and expressed as pg/mL protein.

2.7. Protein Content and Western Blotting (WB) Analysis

Protein content was evaluated using the Lowry et al. method with bovine serum albumin (BSA) as a reference [48]. WB analysis was carried out in accordance with the manufacturer's instructions (Invitrogen, Carlsbad, CA, USA) and a previous report [44]. Briefly, the proteins were subjected to electrophoresis using 4–20% SDS-PAGE gels, followed by electro-transfer onto nitrocellulose membranes. After blocking the membranes with 5% nonfat milk, the membranes were subjected to immunoblot analysis by allowing them to lie overnight with primary antibodies of rabbit polyclonal anti-APP (Invitrogen, Camarillo, CA, USA, catalog number: 51-2700; 1:1000 dilution) and anti-tubulin to normalize the amount of protein loaded (Invitrogen, Camarillo, CA, USA, catalog number: 32-2600; dilution: dilution 1:4000). The blots were washed with PBS and then analyzed using goat anti-rabbit or goat anti-mouse secondary antibodies that were conjugated with horseradish peroxidase (dilution, 1:100,000; A32735; Invitrogen, Camarillo, CA, USA). The visualization of protein bands was achieved through the utilization of a chemiluminescence reagent (ECL Plus), followed by exposure on X-ray film (Kodak, Rochester, NY, USA). The intensity levels of the bands were assessed utilizing the alpha imager gel documentation system (FluorChem E; Cell Biosciences, Santa Clara, CA, USA), with β-tubulin serving as a loading control.

2.8. Immunocytochemistry

The protocol was followed as described previously [40]. Briefly, brain sections were prepared by deparaffinizing them and then washing them with 0.1 M phosphate-buffered saline (PBS) for a duration of 3–10 min. Following this, the sections were incubated in a blocking solution consisting of PBS with 0.3% Triton X-100, 0.1% BSA, and 2% normal goat serum for a period of 2 h at room temperature. Blocking was followed by overnight incubation at 4 °C with moderate shaking in a polyclonal rabbit antibody to β-amyloid 42 (1:1000, Invitrogen, Carlsbad, CA, USA). Sections were then washed twice in PBS and then incubated with horseradish peroxidase-conjugated goat anti-rabbit IgG (Invitrogen, 1:1000) for 1 h to detect immunoreactivity. Following incubation, sections were washed three times in PBS, and 100 µL of 3,3′-diaminobenzidine (DAB) color reagent solution was added. The immunoreaction response was observed under a microscope. With 0.1% Cresyl violet (Nissl stain), the sections were counterstained. Alcohol gradients were used to dehydrate sections, which were then sealed with neutral adhesive. Positive staining was identified as the appearance of brown DAB reaction products.

2.9. Statistical Analysis

The findings are represented as means ± standard error of the mean (S.E.M). Group differences in behavioral studies were analyzed using two-way analysis of variance (ANOVA) with repeated measures. WB and biochemical data were analyzed with one-way analysis of variance (ANOVA) and Bonferroni's post hoc test for multiple comparisons using GraphPad Prism (version 6.0; GraphPad Software, Inc., La Jolla, CA, USA). All groups were compared with each other for every parameter. In every experiment, $p < 0.05$ was set to be statistically significant.

3. Results

3.1. Effect of DTZ on Body Weight Changes in ICV-STZ-Induced Rats

ICV-STZ (3 mg/kg, p.o.) alone treated rat group showed a significant ($p < 0.05$) decrease in body weight as compared to the control values (from 232.72 ± 14.54 g to 165.28 ± 13.24 g). Treatment with indicated doses of DTZ (10, 20, and 40 mg/kg) restored the body weight changes significantly ($p < 0.05$ at 20 and 40 mg/kg) when compared with ICV-STZ-induced rat groups (175.98 ± 18.94 g, 188.92 ± 10.58 g and 205.86 ± 12.55 g at 10, 20 and 40 mg/kg, respectively). Treatment with the standard drug DON (0.1 mg/kg) to ICV-STZ-induced rats also significantly ($p < 0.05$) improved the altered body weights (208.28 ± 11.86 g) and is comparable with DTZ treated at 40 mg/kg dose (Figure 2A).

3.2. Effect of DTZ on Cognitive Deficits in Passive Avoidance Task

To measure the effect of DTZ on ICV-STZ-induced learning and memory impairment in rat groups, acquisition latency (AL) and retention latency (RL) were measured. One day after the treatment schedule (day 22), the AL was unchanged in all the groups. On the following day (day 23), the RL was significantly ($p < 0.001$) decreased in the ICV-STZ-induced group when compared with the control group (from 554 ± 22 s to 248 ± 39 s). Treatment with DTZ at indicated doses (10, 20, and 40 mg/kg) significantly ($p < 0.05$ at 20 and 40 mg/kg).) and dose-dependently attenuated the RL values (270 ± 45 s, 376 ± 36 s and 452 ± 31 s at 10, 20 and 40 mg/kg, respectively) when compared with ICV-STZ treated groups indicating that DTZ significantly improved the cognitive functions. DON treated at 0.1 mg/kg showed similar significant effects (468 ± 19 s, $p < 0.05$) when compared with DTZ in attenuating the ICV-STZ-induced decrease in RL values (Figure 2B).

3.3. Effect of DTZ on ICV-STZ-Induced Cognitive Impairment in MWM Task

The escape latency to locate the hidden platform decreased during the course of the five training trials for the MWM task as compared to day one. ICV-STZ-induced rat group showed a significant ($p < 0.05$) increased average latency in finding the hidden platform when compared to the control group indicating reduced learning and memory capacities

in ICV-STZ-induced rats (16 ± 3 s to 48 ± 4 s on day 5). Treatment with indicating doses of DTZ (10, 20 and 40 mg/kg) or standard drug DON (0.1 mg/kg) decreased the escape latency compared with ICV-STZ alone treated group 42 ± 3 s, 28 ± 4 s, 18 ± 3 s at 10, 20 and 40 mg/kg DTZ and 17 ± 4 s at 0.1 mg/kg DON). Similar effects were observed with DON (0.1 mg/kg) when compared with the DTZ (40 mg/kg)-treated group (Figure 3A). Further, the spatial probe test evaluated by the time spent in the target quadrant after the removal of the hidden platform revealed a significant decrease ($p < 0.05$) in the ICV-STZ-induced group when compared with the control group (from 48 ± 3 s to 27 ± 4 s). Treatment with DTZ to ICV-STZ-induced rats at indicated doses significantly increased ($p < 0.05$ at 20 and 40 mg/kg) the amount of time spent in the target quadrant area, indicating an increase in memory consolidation and learning performance (29 ± 3 s, 34 ± 2 s and 39 ± 1 s at 10, 20 and 40 mg/kg, respectively). DON treatment also exhibited a significant ($p < 0.05$) effect in ameliorating the ICV-STZ-induced memory and learning deficits in both escape latency and probe test and is comparable with DTZ at 40 mg/kg dose (Figure 3B).

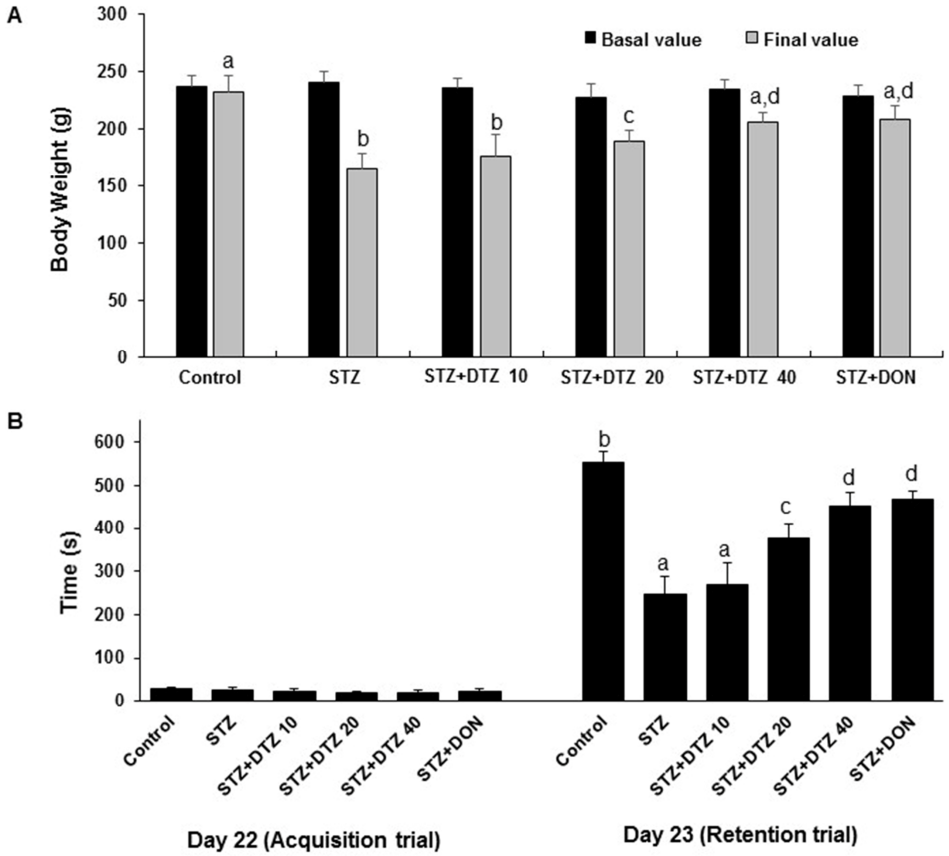


Figure 2. Effect of DTZ on body weight and passive avoidance task in ICV-STZ-induced rats. (**A**) Body weight changes. (**B**) Acquisition trial and retention trial in passive avoidance task. A maximum of 600 s of latency time was measured. Values are expressed as means ± S.E.M (n = 12). The groups of control, STZ, and different concentrations of DTZ or DON were compared with each other. Bars with no common letters are significantly different among groups ($p < 0.05$). STZ: streptozotocin (3 mg/kg), STZ + DTZ 10: diltiazem (10 mg/kg) plus streptozotocin (3 mg/kg) injected group, STZ + DTZ 20: diltiazem (20 mg/kg) plus streptozotocin (3 mg/kg) injected group, STZ + DTZ 40: diltiazem (40 mg/kg) plus streptozotocin (3 mg/kg) injected group, STZ + DON: donepezil (0.1 mg/kg) plus streptozotocin (3 mg/kg) injected group.

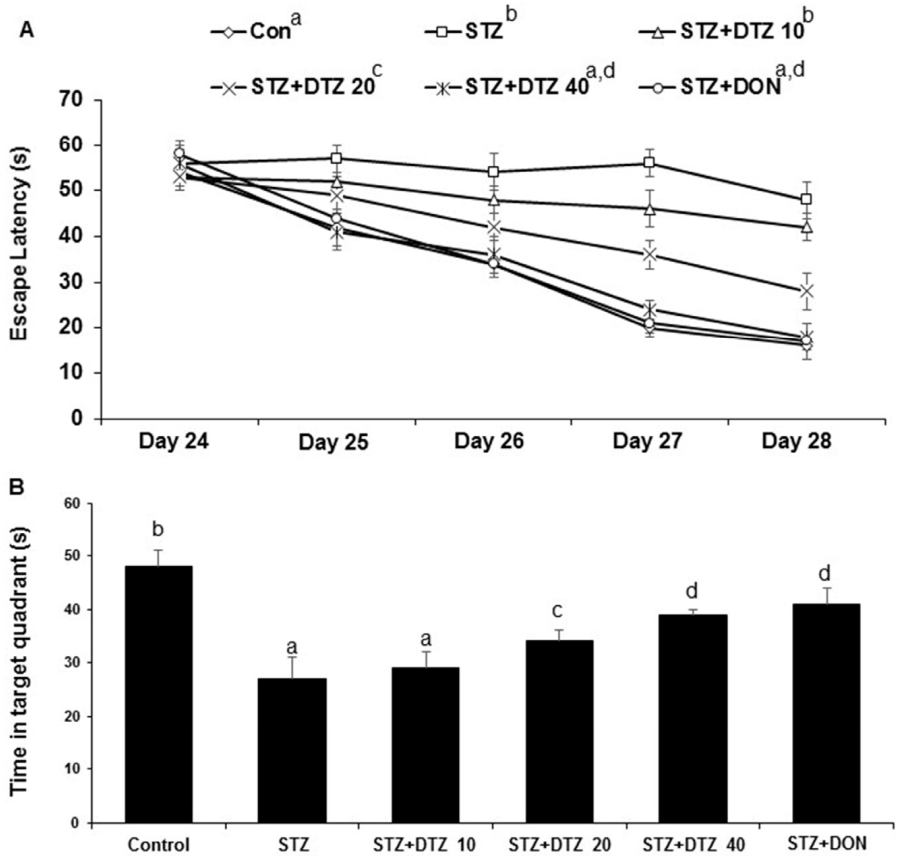


Figure 3. Effect of DTZ in ICV-STZ-induced rat memory performance in MWM task. (**A**) MWM escape latency in ICV-STZ rats. (**B**) The time that ICV-STZ-induced rats spent in the target area. Values are shown as means ± S.E.M (n = 12). The groups of control, STZ, and different concentrations of DTZ or DON were compared with each other. Bars with no common letters are significantly different among groups ($p < 0.05$). STZ: streptozotocin (3 mg/kg), STZ + DTZ 10: diltiazem (10 mg/kg) plus streptozotocin (3 mg/kg) injected group, STZ + DTZ 20: diltiazem (20 mg/kg) plus streptozotocin (3 mg/kg) injected group, STZ + DTZ 40: diltiazem (40 mg/kg) plus streptozotocin (3 mg/kg) injected group, STZ+DON: donepezil (0.1 mg/kg) plus streptozotocin (3 mg/kg) injected group.

3.4. Effect of DTZ on the Anti-Oxidative Enzyme Status in ICV-STZ-Induced Rat Brain Tissues

The oxidative damage caused by ICV-STZ injection was evaluated by measuring the anti-oxidative LPO, GSH, and SOD enzyme levels in rat brain tissues (Figure 4). The LPO enzyme status as measured by TBARS content was significantly ($p < 0.05$) increased in ICV-STZ-induced rat brain tissues when compared with control samples (17.75 ± 2.74 to 26.78 ± 2.12 nM/mg protein). However, DTZ treatment to ICV-STZ-induced rats at indicated doses (10, 20, and 40 mg/kg) reduced the increased TBARS content significantly ($p < 0.05$ at 20 and 40 mg/kg) in a dose-dependent fashion (25.02 ± 3.14, 23.60 ± 1.85 and 20.68 ± 1.82 nM/mg protein at 10, 20 and 40 mg/kg, respectively; Figure 4A). Further, the GSH and SOD enzyme levels showed a significant ($p < 0.05$) decrease in ICV-STZ-induced brain tissues when compared to the control groups (from 28.22 ± 2.45 to 11.24 ± 1.76 for GSH, from 49.46 ± 2.78 to 14.20 ± 1.74 for SOD). Treatment with DTZ (10, 20, and 40 mg/kg) improved the depleted GSH and SOD levels in brain tissues when compared with ICV-STZ-treated rats ($p < 0.05$ at 10, 20, and 40 mg/kg). The standard drug DON (0.1 mg/kg) also lowered the levels of LPO, GSH, and SOD enzymes significantly ($p < 0.05$), and the result was similar as DTZ at 40 mg/kg (Figure 4B,C). Considering the results obtained, DTZ has the potential to regulate the anti-oxidative enzyme status disrupted by ICV-STZ injections in SAD-type rats.

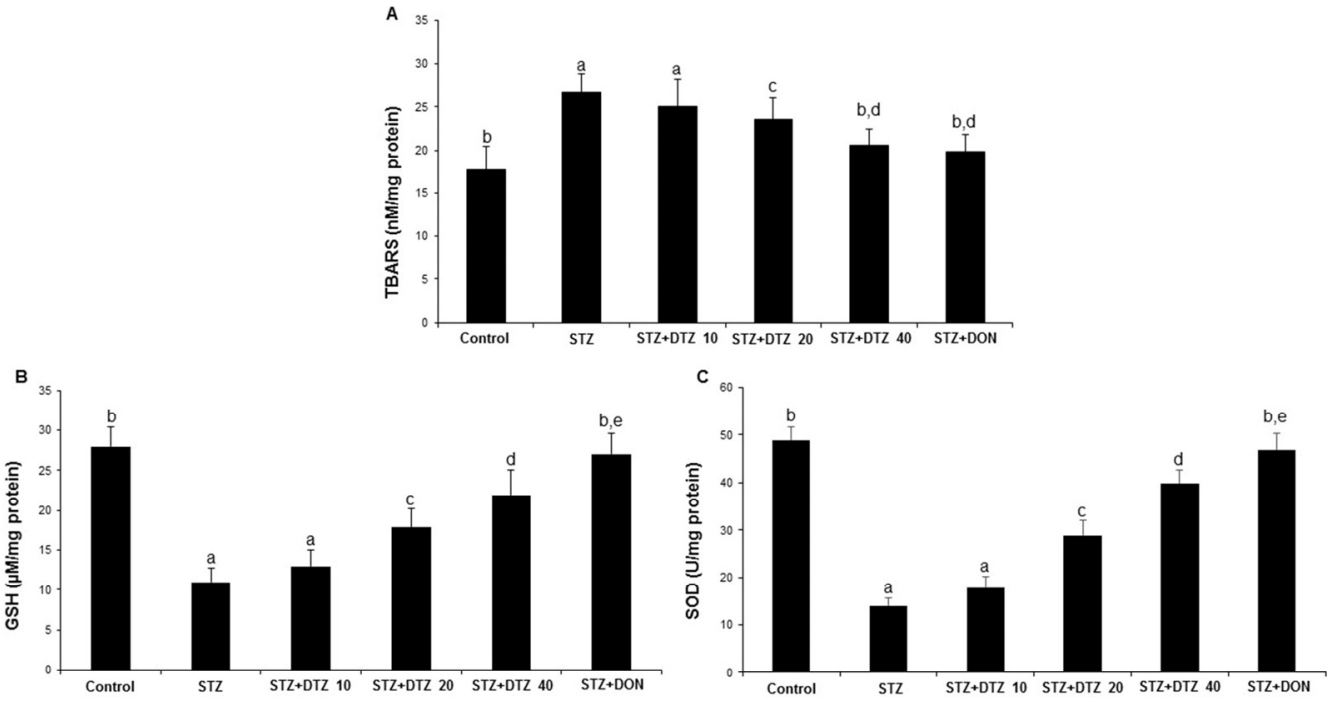


Figure 4. Effect of DTZ on brain anti-oxidative parameters in ICV-STZ-induced rat brain homogenates. (**A**) Lipid peroxidation (LPO) as measured by TBARS, (**B**) Glutathione (GSH) levels, (**C**) Superoxide dismutase (SOD) levels. Values are expressed as mean ± S.E.M, n = 6. The groups of control, STZ, and different concentrations of DTZ or DON were compared with each other. Bars with no common letters are significantly different among groups ($p < 0.05$). STZ: streptozotocin (3 mg/kg), STZ + DTZ 10: diltiazem (10 mg/kg) plus streptozotocin (3 mg/kg) injected group, STZ + DTZ 20: diltiazem (20 mg/kg) plus streptozotocin (3 mg/kg) injected group, STZ + DTZ 40: diltiazem (40 mg/kg) plus streptozotocin (3 mg/kg) injected group, STZ+DON: donepezil (0.1 mg/kg) plus streptozotocin (3 mg/kg) injected group.

3.5. Effect of DTZ on the Pro-Inflammatory Markers in Rat Brain Tissues

To identify the neuroinflammatory protective role of DTZ, the nitrite levels and the pro-inflammatory cytokines (TNF-α and IL-1β) in rat brain tissues were estimated (Figure 5). ICV-STZ-induced rat groups produced a significant increase in brain nitrite levels when compared with the control samples (15.26 ± 1.78 to 36.28 ± 2.24 µM/mg protein; Figure 5A). Similarly, the TNF-α and IL-1β levels were also significantly increased in ICV-STZ-induced groups when compared with control groups (18.65 ± 2.87 to 57.64 ± 3.12 and 6.64 ± 0.87 to 19.76 ± 1.24 pg/mg protein for TNF-α and IL-1β, respectively; Figure 5B,C). Treatment with DTZ at indicated concentrations (10, 20, and 40 mg/kg) significantly ($p < 0.05$ at 20 and 40 mg/kg) attenuated the increased brain TNF-α and IL-1β levels as compared to ICV-STZ-induced rats. DON (0.1 mg/kg)-treated groups also significantly ($p < 0.05$) reduced the increased nitrite, TNF-α, and IL-1β levels (18.24 ± 1.24 µM/mg protein, 24.18 ± 3.02 and 8.78 ± 1.89 pg/mg protein, respectively) and are comparable with DTZ at 40 mg/kg.

3.6. Effect of DTZ on the Total Protein Content and APP Expression

ICV-STZ-induced rats showed a significant decrease ($p < 0.05$) in brain total protein level when compared to the control group. Treatment with DTZ (10, 20 and 40 mg/kg) and DON (0.1 mg/kg) significantly ($p < 0.05$) and dose-dependently (14.26 ± 1.97, 19.56 ± 1.22, 23. 54 ± 1.68 and 24. 68 ± 1.44 µM/mg protein, respectively) prevented ICV-STZ-induced decrease in brain total protein level (Figure 6A). Further, to understand the effect of DTZ on the Aβ protein, the expression of APP processing was analyzed by WB. In ICV-STZ-induced rats, the expression of APP in brain samples was markedly increased when compared with the control group samples. Treatment with DTZ (10, 20, and 40 mg/kg)

suppressed the increased APP expression when compared with the ICV-STZ-induced group. DTZ at 40 mg/kg dose exhibited a similar effect with DON treated at 0.1 mg/kg dose. Densitometry analysis revealed a significant ($p < 0.05$) increase in APP expression rate (1.84 ± 0.15) in ICV-STZ-induced rat brain tissues, and DTZ treatment ameliorated (1.12 ± 0.09) the changes significantly ($p < 0.05$ at 40 mg/kg). DON treatment to ICV-STZ-induced rats also showed a similar effect in attenuating the APP expression rate (1.17 ± 0.15) and is comparable with DTZ treated at 40 mg/kg dose (Figure 6B).

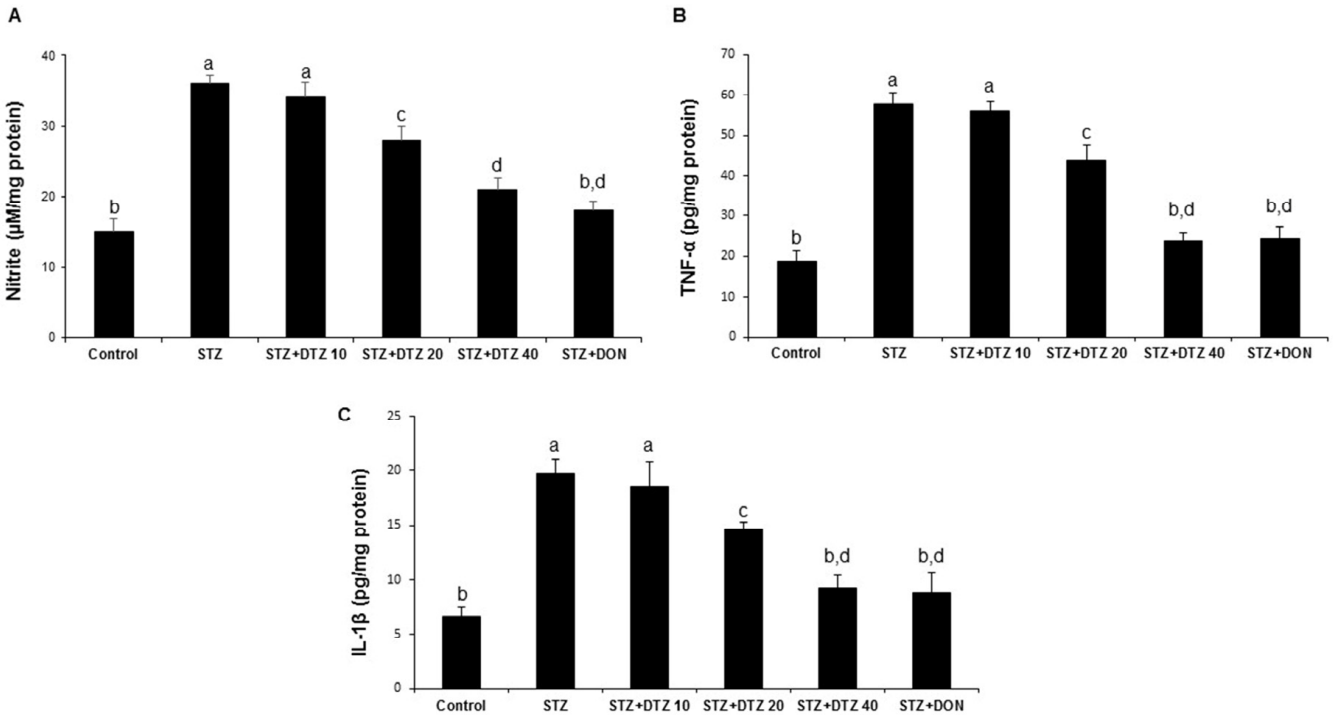


Figure 5. Effect of DTZ on the nitrite and pro-inflammatory cytokines in ICV-STZ-induced rat brain tissues. (**A**) nitrite levels, (**B**) TNF-α levels and (**C**) IL-1β. Values are expressed as mean ± S.E.M, n = 6. The groups of control, STZ, and different concentrations of DTZ or DON were compared with each other. Bars with no common letters are significantly different among groups ($p < 0.05$). STZ: streptozotocin (3 mg/kg), STZ + DTZ 10: diltiazem (10 mg/kg) plus streptozotocin (3 mg/kg) injected group, STZ + DTZ 20: diltiazem (20 mg/kg) plus streptozotocin (3 mg/kg) injected group, STZ + DTZ 40: diltiazem (40 mg/kg) plus streptozotocin (3 mg/kg) injected group, STZ + DON: donepezil (0.1 mg/kg) plus streptozotocin (3 mg/kg) injected group.

3.7. Effect of DTZ on ICV-STZ-Induced Aβ Accumulation in Rat Brain Tissues

To evaluate the presence of Aβ accumulation, immunostaining was carried out using the polyclonal rabbit antibody to β-amyloid 42, which detects the Aβ peptide signal (Figure 7). Marked brown reaction products (DAB) in hippocampal areas were observed in ICV-STZ-induced rat groups when compared with control brain samples, indicating a strong reaction with Aβ antibodies. In DTZ-treated rats exposed to ICV-STZ injections, the Aβ peptide signal was reduced with increasing concentrations. DON treated at 0.1 mg/kg also markedly reduced the Aβ signal exhibiting similar effects as that of DTZ treated at 40 mg/kg dose (Figure 7A–F). Mean density values revealed a significant ($p < 0.05$) increase in the immunoreactivity (0.292 ± 0.004) in ICV-STZ-induced sections when compared with control groups (0.168 ± 0.002). Treatment with DTZ ameliorated these changes in a concentration-dependent manner (0.273 ± 0.006, 0.225 ± 0.005, and 0.163 ± 0.003 at 10, 20 and 40 mg/kg, respectively). DON treatment also exhibited a marked effect in attenuating the immunoreactivity in brain tissue sections (0.181 ± 0.004), and the significance levels are similar with DTZ-treated at 40 mg/kg dose (Figure 7G). The results suggest that the SAD-

type pathologies induced by ICV-STZ injection were ameliorated by DTZ by promoting the clearance of soluble intracellular Aβ deposits, which are the major hallmarks of AD.

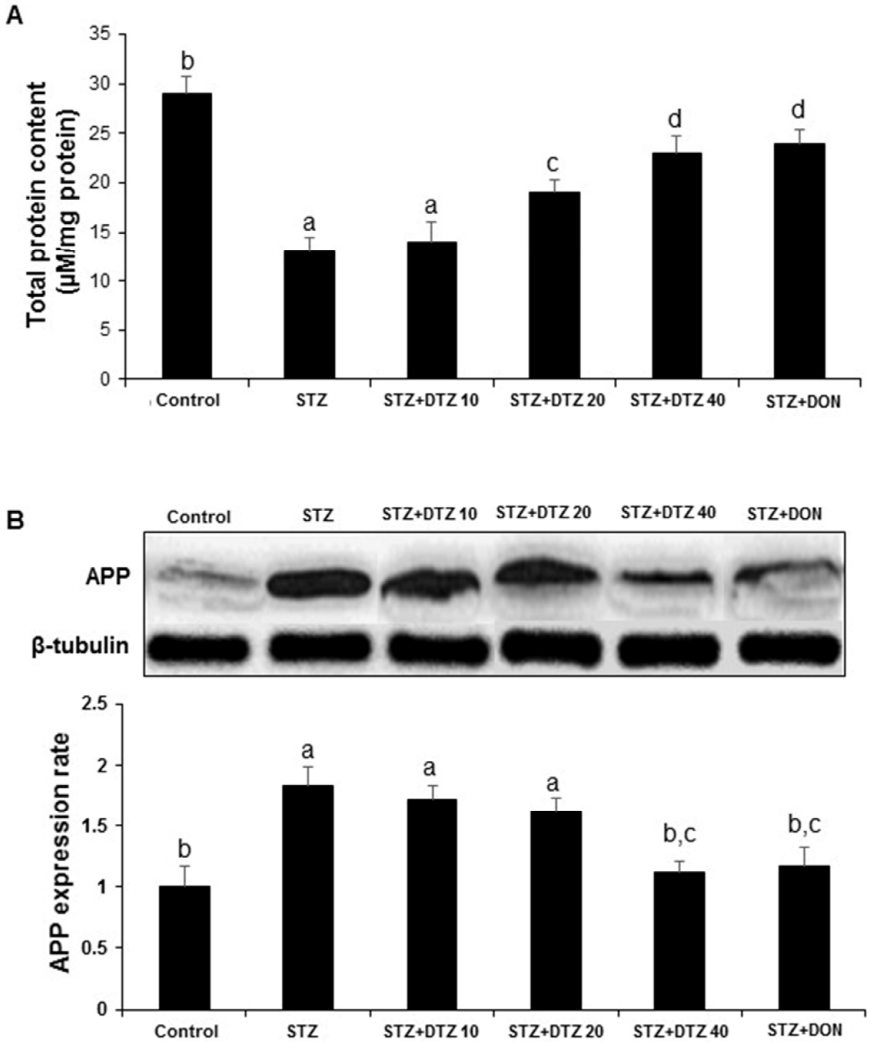


Figure 6. Influence of DTZ on APP expression and total protein content in ICV-STZ-induced brain tissues. (**A**) Total protein content was measured in brain homogenates four weeks after ICV-STZ injection. (**B**) Immunoblot and image analysis were used to measure the amount of APP in rat brain homogenates (lower panel). β-tubulin was used as loading control. Values are shown as means ± S.E.M (n = 6). The groups of control, STZ, and different concentrations of DTZ or DON were compared with each other. Bars with no common letters are significantly different among groups ($p < 0.05$). APP: Amyloid β precursor protein, STZ: streptozotocin (3 mg/kg), STZ + DTZ 10: diltiazem (10 mg/kg) plus streptozotocin (3 mg/kg) injected group, STZ + DTZ 20: diltiazem (20 mg/kg) plus streptozotocin (3 mg/kg) injected group, STZ + DTZ 40: diltiazem (40 mg/kg) plus streptozotocin (3 mg/kg) injected group, STZ+DON: donepezil (0.1 mg/kg) plus streptozotocin (3 mg/kg) injected group.

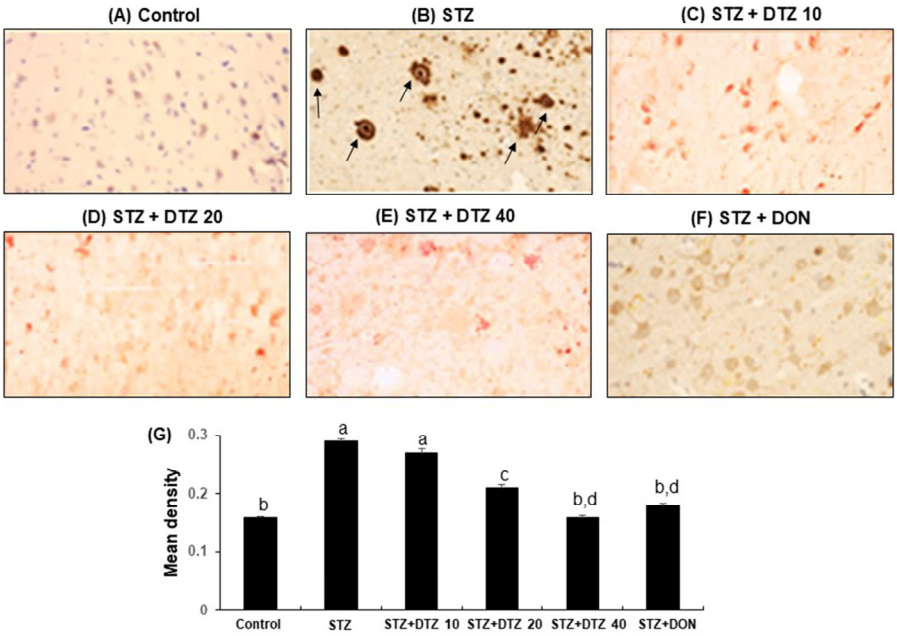


Figure 7. Influence of DTZ on immunohistostaining in ICV-STZ-induced rats. (**A**) Control group, (**B**) ICV-STZ injected group (3 mg/kg), (**C**) DTZ (10 mg/kg) plus ICV-STZ (3 mg/kg) injected group, (**D**) DTZ (20 mg/kg) plus ICV-STZ (3 mg/kg) injected group, (**E**) DTZ (40 mg/kg) plus ICV-STZ (3 mg/kg) injected group, (**F**) DON (0.1 mg/kg) plus ICV-STZ (3 mg/kg) injected group. The brown reactive substances (DAB), as depicted in arrows, indicated substantial amyloid deposition in ICV-STZ-induced group and weak staining was observed in DTZ (10, 20 and 40 mg/kg) and DON (0.1 mg/kg) treated groups. (**G**) Quantitative analysis showing mean density values. Values are expressed as means ± S.E.M (n = 6). The groups of control, STZ, and different concentrations of DTZ or DON were compared with each other. Bars with no common letters are significantly different among groups ($p < 0.05$). Nissl counterstain. Scale as 100 µM. Magnification 200×. ICV-STZ: intra-cerebroventricular-streptozotocin, DTZ: diltiazem, DON: donepezil.

4. Discussion

DTZ has been shown to be effective in the treatment of hypertension, angina, and cardiovascular disease [49,50]. DTZ exerts vasodilatory actions on arterial blood vessels and raises the sympathetic response reflex [51]. A decrease in blood pressure and an increase in cardiac output, heart rate, and contractility are considered to be the main effects of DTZ on cardiovascular disorders [26]. Previous studies have indicated the potential neurological effects of CCBs by regulating or blocking the neuronal voltage-gated calcium channels [10,52]. Further, the neuroprotective potential of CCBs in disorders such as AD, PD, focal cerebral ischemia, and spinal cord ischemia-reperfusion injury was well documented, indicating that CCBs can be used as potential repurposing or repositioning agents for various CNS disorders [17,28,53–55]. In a recent study, CCBs were shown to exert greater potential in the treatment of psychiatric and neurodegenerative disorders and suggested that repurposing trials using the existing CCBs might increase the choice of drug selection for neuroprotection [56]. In this study, DTZ exhibited a beneficial role against the ICV-STZ-induced SAD rats in various aspects by attenuating the altered cognitive deficits, anti-oxidative defense parameters, pro-inflammatory cytokines, and APP expression. In experimental animal models, DTZ has been utilized in a variety of doses ranging from 5 mg/kg to 800 mg/kg for up to 10–40 days [57–59]. In this study, the treatment doses employed (10, 20, and 40 mg/kg) were selected after performing the pilot study and referring to the previous reports [29].

Earlier studies indicated that a single ICV-STZ injection (3 mg/kg) to rodents exhibited cognitive impairments and altered other important oxidative and inflammatory biochemical parameters simulated like that are seen in SAD-like pathology in human AD

patients [36,37,60]. In agreement, a single ICV-STZ injection into rats induced significant pathological alterations by impairing the learning and memory functions in rats as evaluated in passive avoidance and MWM tasks. The latency time to enter the dark chamber was reduced significantly, indicating cognitive deficits in ICV-STZ-induced rats. In the MWM task, increased escape latency time was observed in ICV-STZ-induced animals, and also a reduced time to spend in the target quadrant was observed. Treatment with DTZ at 20 and 40 mg/kg doses attenuated these changes in both passive avoidance and MWM task, indicating a significant improvement in cognitive function disrupted by ICV-STZ injection. Our data agreed with earlier published works wherein DTZ at 40 mg/kg dose ameliorated the cognitive deficits induced by aluminum chloride in experimental mice [29].

Oxidative stress via the excessive production of ROS is known to be one of the important pathological hallmarks of brain aging and AD. Evidence suggests that STZ-induced experimental animals negatively affect the anti-oxidative stress-related enzymatic status leading to free radical-mediated AD progression [60,61]. Further, elevated calcium levels cause oxidative damage, mitochondrial overload, Aβ production, and tau phosphorylation [62]. Increased Aβ further interacts with Fe^{2+} and Cu^{2+} to generate reactive oxygen species (ROS), and ROS leads to lipid peroxidation and altered anti-oxidative enzyme status [63].

In this study, the anti-oxidative enzymatic parameters, including LPO, GSH, and SOD, were estimated in brain tissues. ICV-STZ-induced rats exhibited an increase in LPO as measured by TBARS levels and decreased the GSH and SOD levels significantly. DTZ at 10, 20, and 40 mg/kg dose-dependently restored the altered enzyme status, which agreed with earlier studies that DTZ significantly attenuated oxidative stress in STZ-induced diabetic rabbits and aluminum chloride-induced oxidative stress in mice [29,64].

Neuroinflammation, due to increased pro-inflammatory responses, is another major causative factor in several neurodegenerative disorders, including AD [65,66]. Pro-inflammatory cytokines, including TNF-α, IL-6, IL-1β, and IL-10, increase the Aβ accumulation and promote abnormal tau phosphorylation [67]. Further, single ICV administration of STZ to experimental animals was known to produce inflammation in the brain by increasing the expression of pro-inflammatory cytokines, including TNF-α, IL-6, and IL-1β [68–70]. It has been reported that inhibitors of Ca^{2+} influx can regulate the excessive production of various pro-inflammatory cytokines and NO [11]. Further, DTZ also showed anti-inflammatory effects by reducing the production of anti-inflammatory responses and inhibiting pro-inflammatory mediators [28,71]. In agreement, STZ-induced excessive production of NO and the pro-inflammatory cytokines (TNF-α, and IL-1β) in the brain tissue was ameliorated by DTZ significantly ($p < 0.001$ at 40 mg/kg dose).

Aβ accumulation, together with neuronal cell death and cognitive impairments, are known to be unique symptoms of AD. Earlier reports revealed that ICV-STZ-induced experimental animals exhibited a marked reduction in overall weight of the brain, memory dysfunction, and Aβ accumulation with increased expression of APP, which are well-known pathological changes linked to SAD [72]. In the present study, ICV-STZ-induced rat brain tissues exhibited an increased expression of APP and Aβ deposition analyzed via WB and immunohistochemistry. Treatment with DTZ (40 mg/kg) showed a significant reduction in APP expression dose-dependently. Further, the appearance of strong brown reaction products (DAB) of Aβ deposition immunoreactive signal, as seen in ICV-STZ-induced groups when compared with the control group, was markedly recovered in DTZ-treated rat groups. Although we found dose-dependent effects with DTZ treated at selected doses (10, 20, and 40 mg/kg), significant effects were observed at 20 and 40 mg/kg doses in the majority of the parameters evaluated. Further, no significant difference was observed with DTZ (40 mg/kg) and standard drug DON (0.1 mg/kg) treatments, and the results were comparable.

5. Conclusions

In conclusion, the calcium channel blocker DTZ exhibited neuroprotective anti-dementia effects in ICV-STZ-induced SAD-type experimental rats. DTZ significantly improved the ICV-STZ-induced behavioral and cognitive impairments. Further, DTZ attenuated the altered oxidative stress parameters and neuroinflammation-related pro-inflammatory cytokines in ICV-STZ-induced rat brain tissues. In addition, DTZ suppressed the increased APP expression and restored the amyloid-β depositions in ICV-STZ-induced brain tissues. This study provided therapeutic importance of DTZ for its benefits in repurposing as a potential agent in the treatment and management of various neurodegenerative disorders, including AD. Although the brain penetrability and CNS effects of DTZ are less clear, utilizing available epidemiologic data and translational science might benefit researchers in unveiling the importance of DTZ in neuroprotection. To gain complete therapeutic benefits of DTZ as a potential repurposed drug for neuroprotection, a detailed multifactorial mechanistic-based study in other models of neurodegeneration with more selective central actions might be quite essential.

Author Contributions: Conceptualization, R.A., E.K.K. and S.K.; methodology, R.A., S.K. and P.K.P.; software, S.K., S.R.K. and R.A.; validation, R.A., E.K.K., P.K.P. and S.K.; formal analysis, S.K. and R.A.; investigation, R.A., S.R.K., P.K.P. and E.K.K.; resources, S.K. and R.A.; data curation, R.A., S.R.K., P.K.P., E.K.K. and S.K.; writing, original draft preparation, R.A. and S.K.; writing, review and editing, S.K., E.K.K. and S.R.K.; visualization, S.K. and R.A.; supervision, R.A. and S.K.; project administration, R.A. and S.K.; funding acquisition, R.A. and S.K. All authors have read and agreed to the published version of the manuscript.

Funding: This research received no external funding.

Institutional Review Board Statement: The animal study protocol was approved by the "Purpose of Control and Supervision of Experiments on Animals (CPCSEA)" guidelines and our Institutional Animal Care and Use Committee (No.: 1358/ac/10/CPCSEA).

Informed Consent Statement: Not applicable.

Data Availability Statement: Data are contained within the article.

Acknowledgments: This work was supported by the Department of Science and Technology (DST), Ministry of Science and Technology, India, New Delhi, and partly by Konkuk University, Republic of Korea.

Conflicts of Interest: The authors declare no conflict of interest.

References

1. Guo, T.; Zhang, D.; Zeng, Y.; Huang, T.Y.; Xu, H.; Zhao, Y. Molecular and Cellular Mechanisms Underlying the Pathogenesis of Alzheimer's Disease. *Mol. Neurodegener.* **2020**, *15*, 40. [CrossRef] [PubMed]
2. Haque, R.U.; Levey, A.I. Alzheimer's Disease: A Clinical Perspective and Future Nonhuman Primate Research Opportunities. *Proc. Natl. Acad. Sci. USA* **2019**, *116*, 26224–26229. [CrossRef] [PubMed]
3. Sajjad, R.; Arif, R.; Shah, A.A.; Manzoor, I.; Mustafa, G. Pathogenesis of Alzheimer's Disease: Role of Amyloid-Beta and Hyperphosphorylated Tau Protein. *Indian J. Pharm. Sci.* **2018**, *80*, 581–591. [CrossRef]
4. Masters, C.L.; Bateman, R.; Blennow, K.; Rowe, C.C.; Sperling, R.A.; Cummings, J.L. Alzheimer's Disease. *Nat. Rev. Dis. Primers* **2015**, *1*, 15056. [CrossRef] [PubMed]
5. Iqbal, K.; Grundke-Iqbal, I. Alzheimer's Disease, a Multifactorial Disorder Seeking Multitherapies. *Alzheimer's Dement.* **2010**, *6*, 420–424. [CrossRef] [PubMed]
6. Chin, E.; Jaqua, E.; Safaeipour, M.; Ladue, T. Conventional Versus New Treatment: Comparing the Effects of Acetylcholinesterase Inhibitors and N-Methyl-D-Aspartate Receptor Antagonist With Aducanumab. *Cureus* **2022**, *14*, e31065. [CrossRef] [PubMed]
7. Durães, F.; Pinto, M.; Sousa, E. Old Drugs as New Treatments for Neurodegenerative Diseases. *Pharmaceuticals* **2018**, *11*, 44. [CrossRef] [PubMed]
8. Godfraind, T. Discovery and Development of Calcium Channel Blockers. *Front. Pharmacol.* **2017**, *8*, 286. [CrossRef] [PubMed]
9. Zornow, M.H.; Prough, D.S. Neuroprotective Properties of Calcium-Channel Blockers. *New Horiz.* **1996**, *4*, 107–114.
10. Kopecky, B.J.; Liang, R.; Bao, J. T-Type Calcium Channel Blockers as Neuroprotective Agents. *Pflugers Arch.* **2014**, *466*, 757–765. [CrossRef]

11. Huang, B.-R.; Chang, P.-C.; Yeh, W.-L.; Lee, C.-H.; Tsai, C.-F.; Lin, C.; Lin, H.-Y.; Liu, Y.-S.; Wu, C.Y.-J.; Ko, P.-Y.; et al. Anti-Neuroinflammatory Effects of the Calcium Channel Blocker Nicardipine on Microglial Cells: Implications for Neuroprotection. *PLoS ONE* **2014**, *9*, e91167. [CrossRef] [PubMed]
12. Lovell, M.A.; Abner, E.; Kryscio, R.; Xu, L.; Fister, S.X.; Lynn, B.C. Calcium Channel Blockers, Progression to Dementia, and Effects on Amyloid Beta Peptide Production. *Oxid. Med. Cell. Longev.* **2015**, *2015*, 787805. [CrossRef] [PubMed]
13. Burgoyne, R.D.; Haynes, L.P. Understanding the Physiological Roles of the Neuronal Calcium Sensor Proteins. *Mol. Brain* **2012**, *5*, 2. [CrossRef] [PubMed]
14. Radulescu, C.I.; Cerar, V.; Haslehurst, P.; Kopanitsa, M.; Barnes, S.J. The Aging Mouse Brain: Cognition, Connectivity and Calcium. *Cell Calcium* **2021**, *94*, 102358. [CrossRef] [PubMed]
15. Yu, J.-T.; Chang, R.C.-C.; Tan, L. Calcium Dysregulation in Alzheimer's Disease: From Mechanisms to Therapeutic Opportunities. *Prog. Neurobiol.* **2009**, *89*, 240–255. [CrossRef] [PubMed]
16. Zündorf, G.; Reiser, G. Calcium Dysregulation and Homeostasis of Neural Calcium in the Molecular Mechanisms of Neurodegenerative Diseases Provide Multiple Targets for Neuroprotection. *Antioxid. Redox Signal.* **2011**, *14*, 1275–1288. [CrossRef] [PubMed]
17. Tan, Y.; Deng, Y.; Qing, H. Calcium Channel Blockers and Alzheimer's Disease. *Neural Regen. Res.* **2012**, *7*, 137–140. [CrossRef]
18. Tong, B.C.-K.; Wu, A.J.; Li, M.; Cheung, K.-H. Calcium Signaling in Alzheimer's Disease & Therapies. *Biochim. Biophys. Acta Mol. Cell Res.* **2018**, *1865*, 1745–1760. [CrossRef]
19. Nimmrich, V.; Eckert, A. Calcium Channel Blockers and Dementia. *Br. J. Pharmacol.* **2013**, *169*, 1203–1210. [CrossRef]
20. Zupan, G.; Mrsić, J.; Simonić, A. Effects of Nicardipine, Felodipine and Nifedipine on Passive Avoidance Behavior of Intact and Hypoxia-Exposed Rats. *Arch. Int. Pharmacodyn. Ther.* **1993**, *325*, 61–69.
21. Župan, G.; Vitezić, D.; Mršić, J.; Matešić, D.; Simonić, A. Effects of Nimodipine, Felodipine and Amlodipine on Electroconvulsive Shock-Induced Amnesia in the Rat. *Eur. J. Pharmacol.* **1996**, *310*, 103–106. [CrossRef] [PubMed]
22. Mason, R.P.; Mak, I.T.; Trumbore, M.W.; Mason, P.E. Antioxidant Properties of Calcium Antagonists Related to Membrane Biophysical Interactions. *Am. J. Cardiol.* **1999**, *84*, 16–22. [CrossRef] [PubMed]
23. Godfraind, T. Antioxidant Effects and the Therapeutic Mode of Action of Calcium Channel Blockers in Hypertension and Atherosclerosis. *Philos. Trans. R. Soc. B Biol. Sci.* **2005**, *360*, 2259–2272. [CrossRef]
24. Das, R.; Burke, T.; Van Wagoner, D.R.; Plow, E.F. L-Type Calcium Channel Blockers Exert an Antiinflammatory Effect by Suppressing Expression of Plasminogen Receptors on Macrophages. *Circ. Res.* **2009**, *105*, 167–175. [CrossRef] [PubMed]
25. Chaffman, M.; Brogden, R.N. Diltiazem. *Drugs* **1985**, *29*, 387–454. [CrossRef] [PubMed]
26. Rodríguez Padial, L.; Barón-Esquivias, G.; Hernández Madrid, A.; Marzal Martín, D.; Pallarés-Carratalá, V.; de la Sierra, A. Clinical Experience with Diltiazem in the Treatment of Cardiovascular Diseases. *Cardiol. Ther.* **2016**, *5*, 75–82. [CrossRef]
27. Paquet-Durand, F.; Gierse, A.; Bicker, G. Diltiazem Protects Human NT-2 Neurons against Excitotoxic Damage in a Model of Simulated Ischemia. *Brain Res.* **2006**, *1124*, 45–54. [CrossRef] [PubMed]
28. Fansa, I.; Altug, M.; Melek, I.; Ucar, E.; Kontas, T.; Akcora, B.; Atik, E.; Duman, T. The Neuroprotective and Anti-Inflammatory Effects of Diltiazem in Spinal Cord Ischaemia–Reperfusion Injury. *J. Int. Med. Res.* **2009**, *37*, 520–533. [CrossRef] [PubMed]
29. Rani, A.; Neha; Sodhi, R.K.; Kaur, A. Protective Effect of a Calcium Channel Blocker "Diltiazem" on Aluminum Chloride-Induced Dementia in Mice. *Naunyn-Schmiedeberg's Arch. Pharmacol.* **2015**, *388*, 1151–1161. [CrossRef]
30. Vallazza-Deschamps, G.; Fuchs, C.; Cia, D.; Tessier, L.-H.; Sahel, J.A.A.; Dreyfus, H.; Picaud, S. Diltiazem-Induced Neuroprotection in Glutamate Excitotoxicity and Ischemic Insult of Retinal Neurons. *Doc. Ophthalmol.* **2005**, *110*, 25–35. [CrossRef]
31. Zhang, J.; Cao, H.; Zhang, Y.; Zhang, Y.; Ma, J.; Wang, J.; Gao, Y.; Zhang, X.; Zhang, F.; Chu, L. Nephroprotective Effect of Calcium Channel Blockers against Toxicity of Lead Exposure in Mice. *Toxicol. Lett.* **2013**, *218*, 273–280. [CrossRef] [PubMed]
32. Mathangi, D.C.; Namasivayam, A. Protective Effect of Diltiazem on Cyanide-Induced Neurotoxicity in Wistar Strain Rats. *Food Chem. Toxicol.* **2004**, *42*, 605–608. [CrossRef] [PubMed]
33. Genkova-Papazova, M.G.; Petkova, B.; Shishkova, N.; Lazarova-Bakarova, M. Effect of the Calcium Channel Blockers Nifedipine and Diltiazem on Pentylenetetrazole Kindling-Provoked Amnesia in Rats. *Eur. Neuropsychopharmacol.* **2001**, *11*, 91–96. [CrossRef] [PubMed]
34. Quartermain, D.; Garcia deSoria, V. The Effects of Calcium Channel Antagonists on Short- and Long-Term Retention in Mice Using Spontaneous Alternation Behavior. *Neurobiol. Learn. Mem.* **2001**, *76*, 117–124. [CrossRef] [PubMed]
35. Kamat, P. Streptozotocin Induced Alzheimer′s Disease like Changes and the Underlying Neural Degeneration and Regeneration Mechanism. *Neural Regen. Res.* **2015**, *10*, 1050. [CrossRef]
36. Moreira-Silva, D.; Vizin, R.; Martins, T.; Ferreira, T.; Almeida, M.; Carrettiero, D. Intracerebral Injection of Streptozotocin to Model Alzheimer Disease in Rats. *Bio-Protocol* **2019**, *9*, e3397. [CrossRef]
37. Grieb, P. Intracerebroventricular Streptozotocin Injections as a Model of Alzheimer's Disease: In Search of a Relevant Mechanism. *Mol. Neurobiol.* **2016**, *53*, 1741–1752. [CrossRef] [PubMed]
38. Villar, M.F.Z.; Hanotte, J.L.; Peralta, F.; Reggiani, P.C. Streptozotocin-induced Sporadic Alzheimer's Disease: Behavioral Effects in Female Rats. *Alzheimer's Dement.* **2021**, *17*, e051339. [CrossRef]
39. Zappa Villar, M.F.; López Hanotte, J.; Falomir Lockhart, E.; Trípodi, L.S.; Morel, G.R.; Reggiani, P.C. Intracerebroventricular Streptozotocin Induces Impaired Barnes Maze Spatial Memory and Reduces Astrocyte Branching in the CA1 and CA3 Hippocampal Regions. *J. Neural Transm.* **2018**, *125*, 1787–1803. [CrossRef]

40. Alluri, R.; Ambati, S.R.; Routhu, K.; Kopalli, S.R.; Koppula, S. Phosphoinositide 3-Kinase Inhibitor AS605240 Ameliorates Streptozotocin-Induced Alzheimer's Disease like Sporadic Dementia in Experimental Rats. *EXCLI J.* **2020**, *19*, 71–85. [CrossRef]
41. Raghavendra, V.; Kulkarni, S.K. Possible Antioxidant Mechanism in Melatonin Reversal of Aging and Chronic Ethanol-Induced Amnesia in plus-Maze and Passive Avoidance Memory Tasks. *Free Radic. Biol. Med.* **2001**, *30*, 595–602. [CrossRef]
42. Morris, R. Developments of a Water-Maze Procedure for Studying Spatial Learning in the Rat. *J. Neurosci. Methods* **1984**, *11*, 47–60. [CrossRef] [PubMed]
43. Buttner, J.E. The Rat Brain in Stereotaxic Coordinates, 3rd Edn. By George Paxinos and Charles Watson. *J. Anat.* **1997**, *191*, 315–317. [CrossRef]
44. Ohkawa, H.; Ohishi, N.; Yagi, K. Assay for Lipid Peroxides in Animal Tissues by Thiobarbituric Acid Reaction. *Anal. Biochem.* **1979**, *95*, 351–358. [CrossRef] [PubMed]
45. Ellman, G.L. Tissue Sulfhydryl Groups. *Arch. Biochem. Biophys.* **1959**, *82*, 70–77. [CrossRef] [PubMed]
46. Durak, I.; Yurtarslanl, Z.; Canbolat, O.; Akyol, Ö. A Methodological Approach to Superoxide Dismutase (SOD) Activity Assay Based on Inhibition of Nitroblue Tetrazolium (NBT) Reduction. *Clin. Chim. Acta* **1993**, *214*, 103–104. [CrossRef] [PubMed]
47. Green, L.C.; Wagner, D.A.; Glogowski, J.; Skipper, P.L.; Wishnok, J.S.; Tannenbaum, S.R. Analysis of Nitrate, Nitrite, and [15N]Nitrate in Biological Fluids. *Anal. Biochem.* **1982**, *126*, 131–138. [CrossRef] [PubMed]
48. Lowry, O.H.; Rosebrough, N.J.; Farr, A.L.; Randall, R.J. Protein Measurement with the Folin Phenol Reagent. *J. Biol. Chem.* **1951**, *193*, 265–275. [CrossRef]
49. Tang, L.; Gamal El-Din, T.M.; Lenaeus, M.J.; Zheng, N.; Catterall, W.A. Structural Basis for Diltiazem Block of a Voltage-Gated Ca 2+ Channel. *Mol. Pharmacol.* **2019**, *96*, 485–492. [CrossRef]
50. Tamargo, J.; Ruilope, L.M. Investigational Calcium Channel Blockers for the Treatment of Hypertension. *Expert Opin. Investig. Drugs* **2016**, *25*, 1295–1309. [CrossRef]
51. Mohanty, P.K.; Sowers, J.R.; Thames, M.D. Effects of Hydrochlorothiazide and Diltiazem on Reflex Vasoconstriction in Hypertension. *Hypertension* **1987**, *10*, 35–42. [CrossRef] [PubMed]
52. Ortner, N.J.; Striessnig, J. L-Type Calcium Channels as Drug Targets in CNS Disorders. *Channels* **2016**, *10*, 7–13. [CrossRef] [PubMed]
53. Pasternak, B.; Svanström, H.; Nielsen, N.M.; Fugger, L.; Melbye, M.; Hviid, A. Use of Calcium Channel Blockers and Parkinson's Disease. *Am. J. Epidemiol.* **2012**, *175*, 627–635. [CrossRef] [PubMed]
54. Tseng, Y.-F.; Lin, H.-C.; Chao, J.C.-J.; Hsu, C.-Y.; Lin, H.-L. Calcium Channel Blockers Are Associated with Reduced Risk of Parkinson's Disease in Patients with Hypertension: A Population-Based Retrospective Cohort Study. *J. Neurol. Sci.* **2021**, *424*, 117412. [CrossRef] [PubMed]
55. Lukic-Panin, V.; Kamiya, T.; Zhang, H.; Hayashi, T.; Tsuchiya, A.; Sehara, Y.; Deguchi, K.; Yamashita, T.; Abe, K. Prevention of Neuronal Damage by Calcium Channel Blockers with Antioxidative Effects after Transient Focal Ischemia in Rats. *Brain Res.* **2007**, *1176*, 143–150. [CrossRef] [PubMed]
56. Colbourne, L.; Harrison, P.J. Brain-Penetrant Calcium Channel Blockers Are Associated with a Reduced Incidence of Neuropsychiatric Disorders. *Mol. Psychiatry* **2022**, *27*, 3904–3912. [CrossRef] [PubMed]
57. Chen, Y.-C.; Wu, C.-T.; Chen, J.-H.; Tsai, C.-F.; Wu, C.-Y.; Chang, P.-C.; Yeh, W.-L. Diltiazem Inhibits Breast Cancer Metastasis via Mediating Growth Differentiation Factor 15 and Epithelial-Mesenchymal Transition. *Oncogenesis* **2022**, *11*, 48. [CrossRef]
58. Zadrożniak, A.; Trojnar, M.; Trojnar, M.; Kimber-Trojnar, Ż.; Dudra-Jastrzębska, M.; Andres-Mach, M.; Łuszczki, J.J. Diltiazem Enhances the Protective Activity of Oxcarbazepine against Maximal Electroshock-Induced Seizures in Mice. *J. Pre-Clin. Clin. Res.* **2008**, *2*, 147–152.
59. De Oliveira Bello Corrêa, F.; Giro, G.; Gonçalves, D.; Spolidorio, L.C.; Orrico, S.R.P. Diltiazem Did Not Induce Gingival Overgrowth in Rats: A Clinical, Histological and Histometric Analysis. *Braz. Oral Res.* **2005**, *19*, 163–168. [CrossRef]
60. Shalaby, M.A.; Nounou, H.A.; Deif, M.M. The Potential Value of Capsaicin in Modulating Cognitive Functions in a Rat Model of Streptozotocin-Induced Alzheimer's Disease. *Egypt. J. Neurol. Psychiatr. Neurosurg.* **2019**, *55*, 48. [CrossRef]
61. Sharma, M.; Gupta, Y.K. Chronic Treatment with Trans Resveratrol Prevents Intracerebroventricular Streptozotocin Induced Cognitive Impairment and Oxidative Stress in Rats. *Life Sci.* **2002**, *71*, 2489–2498. [CrossRef] [PubMed]
62. Ge, M.; Zhang, J.; Chen, S.; Huang, Y.; Chen, W.; He, L.; Zhang, Y. Role of Calcium Homeostasis in Alzheimer's Disease. *Neuropsychiatr. Dis. Treat.* **2022**, *18*, 487–498. [CrossRef] [PubMed]
63. Cheignon, C.; Tomas, M.; Bonnefont-Rousselot, D.; Faller, P.; Hureau, C.; Collin, F. Oxidative Stress and the Amyloid Beta Peptide in Alzheimer's Disease. *Redox Biol.* **2018**, *14*, 450–464. [CrossRef] [PubMed]
64. Anjaneyulu, M.; Chopra, K. Diltiazem Attenuates Oxidative Stress in Diabetic Rats. *Ren. Fail.* **2005**, *27*, 335–344. [CrossRef] [PubMed]
65. Heneka, M.T.; Carson, M.J.; El Khoury, J.; Landreth, G.E.; Brosseron, F.; Feinstein, D.L.; Jacobs, A.H.; Wyss-Coray, T.; Vitorica, J.; Ransohoff, R.M.; et al. Neuroinflammation in Alzheimer's Disease. *Lancet Neurol.* **2015**, *14*, 388–405. [CrossRef] [PubMed]
66. Dubey, L. Anti-Inflammatory Action of Diltiazem in Patients with Unstable Angina. *Postgrad. Med. J.* **2006**, *82*, 594–597. [CrossRef] [PubMed]
67. Domingues, C.; da Cruz e Silva, O.A.B.; Henriques, A.G. Impact of Cytokines and Chemokines on Alzheimer's Disease Neuropathological Hallmarks. *Curr. Alzheimer Res.* **2017**, *14*, 870–882. [CrossRef] [PubMed]

68. Wrona, D.; Majkutewicz, I.; Świątek, G.; Dunacka, J.; Grembecka, B.; Glac, W. Dimethyl Fumarate as the Peripheral Blood Inflammatory Mediators Inhibitor in Prevention of Streptozotocin-Induced Neuroinflammation in Aged Rats. *J. Inflamm. Res.* **2022**, *15*, 33–52. [CrossRef] [PubMed]
69. Mishra, S.K.; Singh, S.; Shukla, S.; Shukla, R. Intracerebroventricular Streptozotocin Impairs Adult Neurogenesis and Cognitive Functions via Regulating Neuroinflammation and Insulin Signaling in Adult Rats. *Neurochem. Int.* **2018**, *113*, 56–68. [CrossRef] [PubMed]
70. Kraska, A.; Santin, M.D.; Dorieux, O.; Joseph-Mathurin, N.; Bourrin, E.; Petit, F.; Jan, C.; Chaigneau, M.; Hantraye, P.; Lestage, P.; et al. In Vivo Cross-Sectional Characterization of Cerebral Alterations Induced by Intracerebroventricular Administration of Streptozotocin. *PLoS ONE* **2012**, *7*, e46196. [CrossRef] [PubMed]
71. Begum, A. Comparative Study of Anti-Inflammatory Property of Calcium Channel Blocker and Aspirin in Albino Rats. *Int. J. Basic Clin. Pharmacol.* **2018**, *8*, 21. [CrossRef]
72. Arora, R.B.; Kumar, K.; Deshmukh, R.R. FK506 Attenuates Intracerebroventricular Streptozotocin-Induced Neurotoxicity in Rats. *Behav. Pharmacol.* **2013**, *24*, 580–589. [CrossRef] [PubMed]

Disclaimer/Publisher's Note: The statements, opinions and data contained in all publications are solely those of the individual author(s) and contributor(s) and not of MDPI and/or the editor(s). MDPI and/or the editor(s) disclaim responsibility for any injury to people or property resulting from any ideas, methods, instructions or products referred to in the content.